Growth factor delivery through electrospun nanofibers in scaffolds for tissue engineering applications

Sambit Sahoo,[1,2] Lay Teng Ang,[1] James Cho-Hong Goh,[1,2] Siew-Lok Toh[1,3]
[1]*Tissue Repair Laboratory, Division of Bioengineering, National University of Singapore, Singapore 117574, Singapore*
[2]*Department of Orthopaedic Surgery, National University of Singapore, Singapore 119074, Singapore*
[3]*Department of Mechanical Engineering, National University of Singapore, Singapore 117576, Singapore*

Received 10 February 2009; revised 26 August 2009; accepted 27 August 2009
Published online 14 December 2009 in Wiley InterScience (www.interscience.wiley.com). DOI: 10.1002/jbm.a.32645

Abstract: Tissue engineering scaffolds should ideally mimic the natural ECM in structure and function. Electrospun nanofibrous scaffolds are easily fabricated and possess a biomimetic nanostructure. Scaffolds can mimic ECM function by acting as a depot for sustained release of growth factors. bFGF, an important growth factor involved in tissue repair and mesenchymal stem cell proliferation and differentiation, is a suitable candidate for sustained delivery from scaffolds. In this study, we present two types of PLGA nanofibers incorporated with bFGF, fabricated using the facile technique of blending and electrospinning (Group I) and by the more complex technique of coaxial electrospinning (Group II). bFGF was randomly dispersed in Group I and distributed as a central core within Group II nanofibers; both scaffolds showed similar protein encapsulation efficiency and release over 1–2 weeks. Although both scaffold groups favored bone marrow stem cell attachment and subsequent proliferation, cells cultured on Group I scaffolds demonstrated increased collagen production and upregulated gene expression of specific ECM proteins, indicating fibroblastic differentiation. The study shows that the electrospinning technique could be used to prolong growth factor release from scaffolds and an appropriately sustained growth factor release profile in combination with a nanofibrous substrate could positively influence stem cell behavior and fate. © 2009 Wiley Periodicals, Inc. J Biomed Mater Res 93A: 1539–1550, 2010

Key words: tissue engineering; biomimetic scaffolds; electrospinning; nanofibers; growth factors

INTRODUCTION

Tissue engineering offers a method of healing injuries that would otherwise require treatment with tissue grafts or prostheses. However, research in this field faces several limitations like the lack of an ideal cell type for engineering various tissues, as well as the lack of ideal scaffolds that could aid and sustain the growth and proliferation of the seeded cells to regenerate the injured tissues. Use of mesenchymal stem cells, derived from replenishable sources like the bone marrow, has an advantage over use of differentiated cells which would require harvesting and enzymatic digestion of healthy tissues from donor sites. However, such stem cells would need to proliferate and then differentiate into the desired phenotype with the aid of adequate chemical, mechanical, or biological stimuli. Biological stimuli like growth factors are commonly used to promote stem cell proliferation and differentiation. In most studies, the growth factors are supplied directly into the culture medium at regular intervals. However, this is feasible only *in vitro* but not in *in vivo* applications, when it is desirable to have a sustained release of bioactive growth factor from the scaffold.

Scaffolds with sustained growth factor release capability are often fabricated using hydrogels.[1] However, hydrogel-based scaffolds have limitations such as cell death in the depths of the scaffolds as well as poor mechanical properties, and can only be used for applications where mechanical properties or uniform 3-D distribution of cells are not of major concern. There is thus a need for development of alternate methods of growth factor delivery in scaffolds. Recently, electrospinning technology has been increasingly used to fabricate nanofibrous scaffolds for tissue engineering of skin, bone, tendon, ligament, cartilage, neurons and blood vessels. These constituent fibers, most commonly referred to as "nanofibers," "submicron range," or "ultrafine" fibers, possess diameters ranging from 100 nm to 5 μm, and consequently have a high surface area to volume ratio, suitable for cell attachment and proliferation. Various cell types including mesenchymal

Correspondence to: S. L. Toh; e-mail: bietohsl@nus.edu.sg

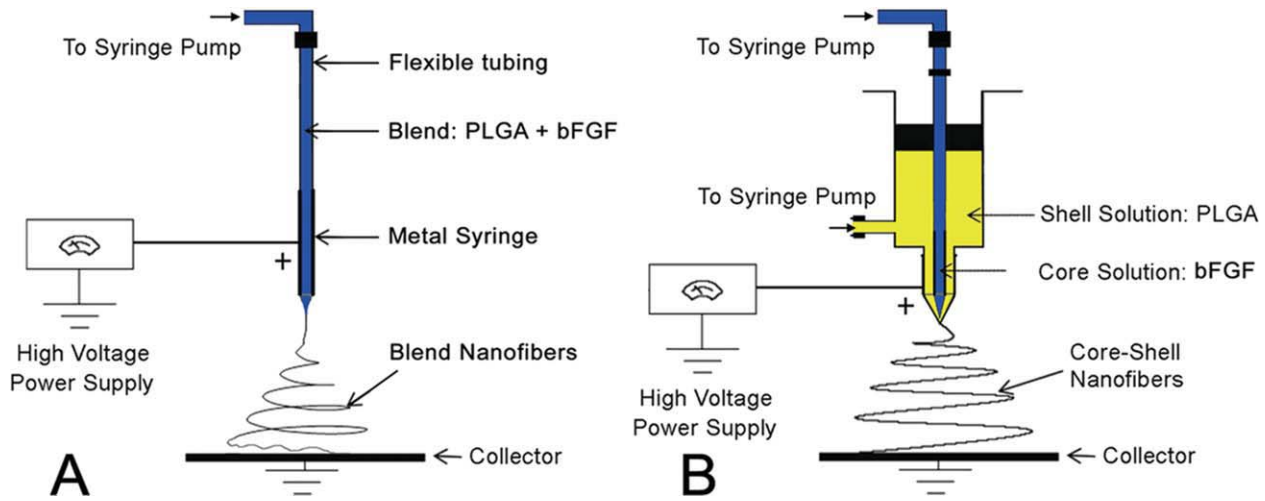

Figure 1. (A) Blend electrospinning setup; (B) coaxial electrospinning setup: "core-shell" structured nanofibers can be electrospun using two different solutions passing through two coaxial needles. [Color figure can be viewed in the online issue, which is available at www.interscience.wiley.com.]

stem cells have been grown successfully on nanofiber scaffolds and such cells also have been induced to differentiate along osteocytic, adipocytic, and chondrocytic lineages.[2,3] Another phenotypic differentiation that is important for engineering of various connective tissues like tendons, ligaments, and skin is fibroblastic differentiation. Among the various growth factors that have been shown to influence fibroblastic differentiation of mesenchymal stem cells, bFGF is a leading candidate, stimulating not only fibroblastic differentiation, but also MSC proliferation and self-renewal.[4] bFGF is known to play an important role in the embryonic development and differentiation of various connective tissues, and also mediates angiogenesis, wound healing and tissue repair.[5,6] However, like most growth factors, bFGF has a very short plasma half-life (90 s), and for optimal effects, it requires repeated local administration. Incorporating bFGF into nanofibers is an attractive way of ensuring continued local release of the growth factor, allowing proliferation and fibroblastic differentiation of the seeded bone marrow stem cells (BMSCs). Generation of such fibrogenic tissues is essential for engineering of ligaments and tendon, which are the research focus of the author's group.[7–11]

The versatility of the electrospinning technique offers a possibility of incorporating protein growth factors within polymer nanofibers, which could then serve as a source of continued and controlled release of the growth factor.[12–16] Coaxial electrospinning, a modification of the electrospinning technique using two concentric needles [Fig. 1(B)] has been used to spin two immiscible solutions into coaxial fibers;[17–19] proteins have been incorporated into the core of such nanofibers.[16,17,20] Such a method protects the protein from the organic solvent used to dissolve the outer polymer coat, and also enables electrospinning of a protein solution that is otherwise not "electrospinnable." While incorporation of growth factors into nanofibers has been attempted before,[12,15] studies on coaxial electrospinning have been mostly limited to model proteins like albumin and lysozyme, with a single study using a growth factor.[14] Moreover, there are no comparative studies on the incorporation and release of growth factors from nanofibers fabricated using conventional electrospinning and coaxial electrospinning.

In this study, we present two modifications of the electrospinning technique to develop bFGF-releasing PLGA nanofibers, fabricated by blending and electrospinning (Group I) or by coaxial electrospinning (Group II). The nanofiber matrices were characterized morphologically, physicochemically and also biologically to evaluate their efficacy for allowing mesenchymal stem cell proliferation and differentiation.

MATERIALS AND METHODS

Scaffold fabrication

Group I nanofibers were fabricated by mixing an aqueous solution of 20 μg of lyophilized bFGF (Raybiotech) in 333 μL of 5 m*M* TRIS (pH 7.6) containing 0.1% Bovine Serum Albumin (BSA; Sigma Aldrich, St. Louis), with 1.5 mL of 6.1% PLGA (PLA85:PGA15; Purac Asia Pacific, Singapore) solution in hexafluoro-2-propanol (HFIP; Fluka Chemie GmBH, Germany). After vortexing for 1 min, this blend was electrospun using a high voltage power supply unit (RR 30-2P/DDPM, Gamma High-Voltage Research,

TABLE I
Protein and PLGA Composition in the Electrospinning Solution(s)

Component	Concentration (%)	Volume (μL)	Weight (mg)
FGF-2	–	{333	0.020
BSA	0.1		0.333
PLGA	6.1	1500	91.50
Total			91.853

Ormond), at 10–12 kV and a flow-rate of 0.45 mL/h, onto several round glass coverslips placed on a grounded collector, about 15 cm from the positively-charged spinneret [Fig. 1(A)].

Group II nanofibers were fabricated by using a coaxial electrospinning set-up [Fig. 1(B)]. Using the same solutions but instead of mixing them as in Group I, the bFGF solution was kept in the inner channel of the set-up and the PLGA solution in the outer channel. Electrospinning was performed at a similar voltage, using a flow-rate of 0.1 mL/h for the inner solution and 0.35 mL/h for the outer solution. The final weight composition of either group of scaffold would be identical as shown in Table I.

Control scaffolds not containing bFGF were also fabricated for both groups by replacing the bFGF solution with 5 m*M* TRIS buffer (pH 7.6) containing 0.1% BSA. The bFGF containing scaffolds are termed (+) and those without are termed as (−) in each group. The scaffolds were vacuum-dried at room temperature overnight and then kept in a desiccator at 4°C until further use.

Scaffold characterization

The scaffolds were characterized for their morphology, protein distribution and hydrophilicity, using a variety of techniques.

i. Scanning electron microscopy. The nanofiber matrices, collected on glass slides for 60 seconds, were sputter-coated with gold at 10 mA, 10 psi for 50–60 s (JFC-1200 Fine Coater, JEOL) and their morphology observed by SEM (JSM-5800LV, JEOL, Tokyo, Japan) at 100 kV accelerating voltage. The images were analyzed by image analysis software (Olympus MicroImage v4.5.1, Olympus Optical, Germany) to determine the diameter distribution of the fibers.
ii. Atomic force microscopy. Nanofibers were collected on mica films for 5 min, and imaged using an AFM (Quartz, Cavendish Instruments, UK); the images were processed and analyzed using MultiView 1000 software (Nanonics Imaging, Israel).
iii. Fluorescence Microscopy. FITC-conjugated BSA (Sigma Aldrich, St. Louis) was used as a model protein to study protein distribution within the nanofibers, collected for 15 s on glass cover slips, by fluorescence microscopy using a laser scanning confocal microscope (LSCM, Leica TCS SP2, Germany).
iv. Static Water Surface Contact Angle. Surface contact angle (SCA; VCA-Optima, AST Products, MA) measurements were performed on the various scaffolds, and also on pure PLGA nanofibrous scaffolds. Since the rough surface of nanofibrous scaffolds could potentially confound SCA measurements, overestimating the hydrophobicity of surfaces, thin films of PLGA and PLGA-BSA blends were also used as additional controls.
v. Attenuated Total Reflectance-Fourier Transform Infrared (ATR-FTIR) Spectroscopy. ATR-FTIR Spectroscopy was performed on the coaxial and blend scaffolds to ascertain the presence of proteins in the nanofibers.
vi. Transmission Electron Microscopy. Transmission Electron Microscopy (TEM, JEOL JEM-2010F) was also performed to further confirm the results after collecting the nanofibers for 15 s on formvar-coated copper grids, carbon-coating and drying in a vacuum oven for 48 h at room temperature before TEM imaging at 100kV.

Protein release kinetics

Nanofibrous scaffolds were collected on 35-mm diameter glass coverslips ($n = 12$, for each group). The nanofiber layer was carefully cut around the coverslips which were weighed before and after electrospinning to estimate the average weight of the nanofiber matrix on each coverslip. The coverslips with nanofiber-matrix were placed in separate wells of four 6-well plates, were incubated in 5 mL of release buffer comprising 1× PBS with 0.1% BSA and 0.01% sodium azide (Fluka Chemie GmBH, Germany), at 37°C over a period of 2 weeks. The nanofiber scaffolds were kept submerged in the wells by using stainless steel rings. After specified intervals (days 1, 3, 7, and 14), the release-medium was collected and the kinetics of bFGF release from the scaffolds ($n = 3$) were analyzed by ELISA using a FGF-2 ELISA kit (Calbiochem, Merck KGaA, Germany).

Efficiency of loading or encapsulation of protein in the nanofibers for the two electrospinning methods was determined by base-surfactant method.[21] Scaffolds of each group ($n = 3$) were dried, weighed and subjected to hydrolysis in 0.1*N* NaOH, 5*M* Urea, 0.08% SDS in 50 m*M* Tris extraction medium at 37°C for 3 h. After neutralization with 0.1*N* HCL and centrifugation, the protein concentration in the supernatant was measured. As bFGF levels after such base-surfactant extraction were below the detection levels of the ELISA kit, total protein content in the supernatant were measured by Bradford microassay. Protein encapsulation efficiency was calculated from the ratio of the protein content in the supernatant to the theoretically obtained total protein content of the electrospun scaffolds.

BMSC isolation and culture

Rabbit BMSCs were isolated and cultured by a previously described protocol,[10] approved by the NUS Institutional Animal Care and Use Committee, National University of Singapore. In brief, bone marrow was aspirated from the iliac crest of anaesthetized New Zealand White Rabbits (NZWR) and collected into polypropylene tubes containing preservative-free heparin (1000 units/mL). The bone marrow was then diluted in an equal volume of

culture medium containing Dulbecco's modified Eagle's medium (DMEM) with low glucose, L-glutamine, 110 mg/L Na-Pyruvate, Pyridoxine HCl (GIBCO, Invitrogen Corporation, CA), fetal bovine serum (15% w/v; GIBCO), and plated into culture flasks. BMSCs were selected by their property of short-term adherence to tissue culture polystyrene, on incubation at 37°C with 5% humidified CO_2. After 24 h, nonadherent cells were discarded and adherent cells cultured, every 3 days medium was changed. When culture flasks became nearly confluent after about 7 days, the cells were detached and serially subcultured. Semiconfluent cells of early (second or third) passage were used for cell seeding experiments.

Cell seeding and culture on scaffolds

Nanofibrous scaffolds, collected over 3 h on 32-mm diameter glass coverslips, were sterilized by exposure to formaldehyde gas for 1 h followed by degassing overnight in the biosafety cabinet. Scaffolds were placed in 6-well plates and seeded with rabbit BMSCs at a density of 10^4 cells/cm^2 in DMEM-High Glucose (Sigma Aldrich) supplemented with 5% FBS and 1% Penicillin-Streptomycin (GIBCO). The constructs were cultured in a 5% CO_2 incubator at 37°C for 2 weeks, with the medium being replaced every 3 days.

Cell seeding efficiency

The cell seeding efficiency was estimated from the proportion of unattached cells in the culture medium, using a method previously described.[10] After incubating the cell-seeded scaffolds ($n = 6$, for each scaffold type) for 18 h, the culture medium was collected from the wells into separate centrifuge tubes. The cell pellets obtained after centrifugation were resuspended in 100 μL of medium and cell count performed. The cell seeding efficiency was expressed as the number of cells attached to the scaffold as percentage of the number of cells seeded.

Live cell staining and SEM imaging of cell proliferation

Fluorescein diacetate (FDA, Molecular Probes, Invitrogen Corporation) was used to stain the live cells on the construct. After removing the culture medium, cell-seeded scaffolds were rinsed with 1× PBS and then incubated in 1 mL 1× PBS supplemented with 2 μL FDA (5 mg/mL) for 30 min at 37°C. After rinsing twice with 1× PBS, the green-stained live cells were visualized using an inverted fluorescence microscope (IX71 Inverted Research Microscope, Olympus) with a blue filter (excitation λ: 480 ± 20 nm, emission λ: 535 ± 25 nm).

For SEM, the samples were rinsed with 1× PBS, fixed with 3.7% formaldehyde for 30 min and then rinsed with tap water. The samples were then dehydrated in graded concentrations of ethanol and then air dried overnight. The dried samples were sputter-coated with gold and observed under the SEM at an accelerating voltage of 15 kV.

Cell proliferation assay

Cell proliferation on the scaffolds was estimated by DNA quantitation using the PicoGreen assay (Molecular Probes, Invitrogen) on the 3rd, 7th, and 14th day of *in vitro* culture. After a cycle of freeze-thawing and freeze-drying, 400 μL of lysis buffer was added to each well and mixed well by pipetting. The lysis buffer was prepared by mixing nine parts of TE buffer from the PicoGreen kit (Molecular Probes, Invitrogen) and one part of RLT Buffer (Qiagen easyRNA extraction kit), supplemented with 1:100 β-mercaptoethanol. The cell-lysate was carefully aspirated into a 1.5 mL microcentrifuge tube, vortexed for 6 min and centrifuged at 13,000 rpm for 10 min. Twenty microliters of the supernatant was added to separate wells in a 96 NUNC black well plate containing 80 μL of prewarmed PicoGreen dye, and mixed by pipetting. Fluorescence intensity at 520 nm wavelength was measured using a microplate reader (FLUOstar OPTIMA, BMG Labtech GmbH, Germany) after excitation at 485 nm, using a gain of 1000, 10 flashes per well, and a position delay time of 0.2–0.5s. BMSC proliferation on TCP in DMEM-HG with 5% FBS was also measured as a control.

Collagen production: Sircol assay

Collagen being one of the key components of the ECM, it is vital that it is produced in abundant amounts by the seeded cells. Moreover, increased collagen production and deposition would also be indicative of stem cell differentiation into a fibroblastic lineage.

On the 3rd, 7th, and 14th day of culture, the total soluble collagen synthesized and secreted into the culture medium was determined by SirCol® Assay (Biocolor, Northern Ireland) using previously described methods.[10] The culture medium was replaced by fresh DMEM with 5% FBS, 2 days before the day of assay, to ensure that only freshly synthesized soluble collagen was assayed. Absorbance of PicroSirius Red stained collagen was read at 540 nm (TECAN Microplate Reader, Magellan Instrument Control and Data Analysis Software) to obtain the concentration of collagen in the medium, which was then multiplied with the total volume of medium collected from the respective scaffolds to give an estimate of the total amount of collagen secreted per scaffold over 2 days. Collagen production from BMSCs grown on TCP in DMEM-HG with 5% FBS was also measured as a control.

Q-RT-PCR analysis for expression of fibrous ECM proteins from BMSCs

In addition to increased proliferation, bFGF is expected to induce fibroblastic differentiation of BMSC and an associated upregulation of gene expression for fibrous ECM proteins. The gene expression of two predominant fibrous ECM proteins, collagen type I and fibronectin, were studied and compared on the two scaffold groups ($n = 3$, for each group).

Total RNA was extracted from day 14 samples of the both scaffolds groups and also from BMSCs cultured on TCP

TABLE II
Real-Time PCR Primers Used in the Study

Primer	Sequence
Collagen I (α2)	F: GCA TGT CTG GTT AGG AGA AAC C
	R: ATG TAT GCA ATG CTG TTC TTG C
Fibronectin	F: CTC ACC CGA GGC GCC ACC TA
	R: TCG CTC CCA CTC CTC TCC AAC G
GADPH	F: GAC ATC AAG AAG GTG GTG AAG C
	R: CTT CAC AAA GTG GTC ATT GAG G
β-Actin	F: CCC ATC TAC GAG GGC TAC G
	R: CCA CGT AGC ACA GCT TCT CC

Primers for collagen type I, GAPDH and β-actin were designed from NZWR gene sequences obtained from GenBank (accession Numbers D49399, NM_001082253 and AF309819, respectively) using Primer3 Software (http://frodo.wi.mit.edu). Primers for fibronectin were obtained from published literature.[22]

under the same culture conditions (DMEM-HG with 5%FBS) using Qiagen RNeasy Kit®. The RNA extract was assessed for its purity and concentration of RNA by spectrophotometry and stored at −80°C. Quantitative or real time RT-PCR (Q-RT-PCR) was performed in duplicate for each sample using SYBR-Green chemistry for collagen Type I and fibronectin, using GAPDH and β-actin as reference genes. The primer sequences (as in Table II) were either obtained from published literature[22] or designed from rabbit gene sequences obtained from the GenBank database, using Primer-3 software, and synthesized by Research Biolabs, Singapore and optimized for PCR efficiency (>90%) and specificity (single peaks on melt curve and single bands of expected molecular weight after electrophoretic separation). Q-RT-PCR was performed using a two-step method wherein cDNA was synthesized from RNA (iScript, Bio-Rad Laboratories, CA) followed by real time PCR expansion (iQ SYBR Green Supermix, Bio-Rad Laboratories, CA) using the specific primers on a iCycler iQ detection system (Bio-Rad Laboratories, CA). Data were analyzed for relative expression using the $\Delta\Delta C_T$ method, after normalization against the expression profile of cells grown on TCP.

Data reduction and statistical analysis

Data were analyzed by single-factor ANOVA and post hoc Tukey tests for multiple comparisons and two-tailed, unpaired Student's *t*-tests for pair-wise comparisons. Results were presented as mean ± standard deviation and $p < 0.05$ was accepted as significant.

RESULTS

Scaffold characterization

Scaffolds of both Group I and II were observed to be composed of continuous nanofibers with similar morphology on SEM and AFM. AFM images obtained on scaffolds (Fig. 2) demonstrated groups of nanofibers of 500–700 nm diameter; such grouping of nanofibers is likely the result of splitting during electrospinning of a single jet into multiple sub-jets, immediately before collection on the substrate. SEM images showed nanofibers with diameter distributed between 100 and 500 nm (Fig. 3). Narrower fiber diameters were obtained from SEM images due to observed fiber shrinkage resulting from thermal degradation of PLGA by the high energy electron beam, especially at higher magnifications.[23]

FTIR studies indicated that protein was incorporated in both groups of nanofibers; the presence of additional peaks at 1635 and 1644 cm^{-1}, corresponding to protein Amide I and at 1534 cm^{-1}, corresponding to protein Amide II is characteristic of proteins (Fig. 4). The peaks were more prominent on the Group I fibers, presumably due to a more superficial arrangement of the proteins on these fibers. All nanofibers had a characteristic peak at 1758 cm^{-1} corresponding to C=O stretch in the PLGA molecule.[24]

Group I scaffolds were less hydrophobic (SCA, 121.1°) than Group II (128.4°) and PLGA-only nanoscaffolds (129.1°). As with rough nanofibrous scaffolds, thin films of the PLGA-protein blend used to fabricate the Group I scaffolds were also less hydrophobic (SCA, 80°) compared to PLGA films (SCA, 94.5°) suggesting that blending resulted in random dispersion and a more superficial distribution of proteins in the nanofibers (Fig. 5). This was confirmed by LSCM and TEM (Fig. 6), which showed a random dispersion of proteins within Group I nanofibers but a "core-shell" structure within Group II nanofibers. While most nanofibers in Group I showed the presence of protein, the distribution of protein in the Group II nanofibers was not continuous and not all fibers possessed the protein core.

Protein release kinetics

Scaffolds collected on 35-mm diameter coverslips had an average weight of 13.5 ± 2.46 mg. Both scaffold groups had a similar protein encapsulation efficiency of 54 ± 5%. Release kinetics results indicate that both scaffolds could sustain a release for 1 week. Compared to Group I scaffolds, which released all the encapsulated bFGF in 7 days, Group II scaffolds could sustain the release till 14 days. The cumulative release profile from the two scaffold groups are plotted in Figure 7.

Cell seeding efficiency and cell proliferation (Live cell staining, SEM, picogreen assay)

More than 90% of the seeded rabbit BMSCs attached onto the scaffolds in 18 h. Better cell proliferation and spreading was observed on bFGF-releasing scaffolds, especially in Group I, by fluorescent

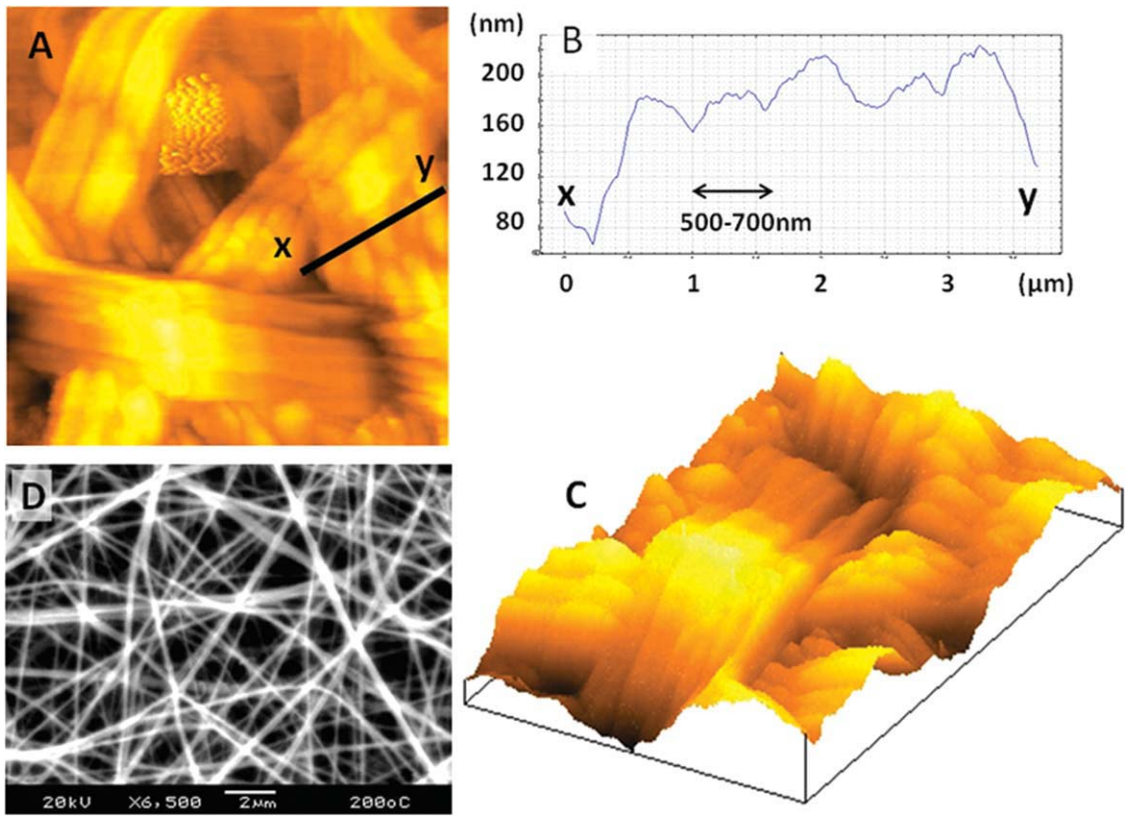

Figure 2. Two-dimensional (A) and three-dimensional (C) AFM images showing Group I nanofibers of 500–700 nm diameter, as measured by profiling along *x-y* (B); SEM image (D) showing fibers ranging in diameter from 100 to 500 nm. [Color figure can be viewed in the online issue, which is available at www.interscience.wiley.com.]

microscopy after live cell staining with FDA and SEM (Fig. 8).

PicoGreen assay corroborated the aforementioned findings showing that the cell population on the Group I (+ and −) scaffolds increased gradually and consistently over the 2 weeks of culture. Scaffolds containing bFGF always showed higher cell proliferation compared to the respective control scaffolds without bFGF. On day 14, Group I (+) scaffolds had significantly higher cell population as compared with Group I (−) scaffolds on the same day; simi-

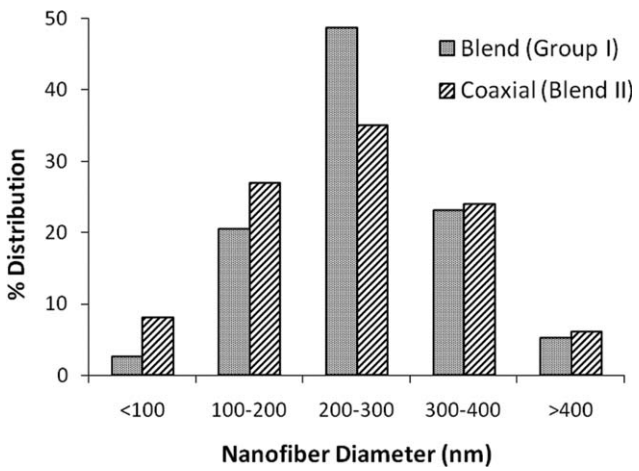

Figure 3. Histogram showing diameter distribution of nanofibers as measured from SEM images. Both Group I and II had 85% of the fibers in 100–500 nm diameter range.

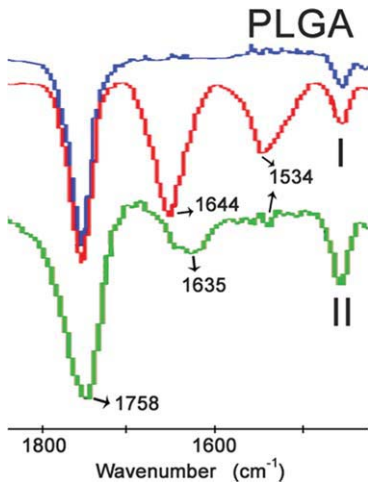

Figure 4. FTIR spectra demonstrating presence of proteins in the Group I (in red) and Group II nanofibers (in green) indicated by characteristic protein Amide-I peaks (1635/1644 cm^{-1}) and protein Amide II peaks (1534 cm^{-1}) that are absent in the spectral plot of pure PLGA nanofibers (in blue). [Color figure can be viewed in the online issue, which is available at www.interscience.wiley.com.]

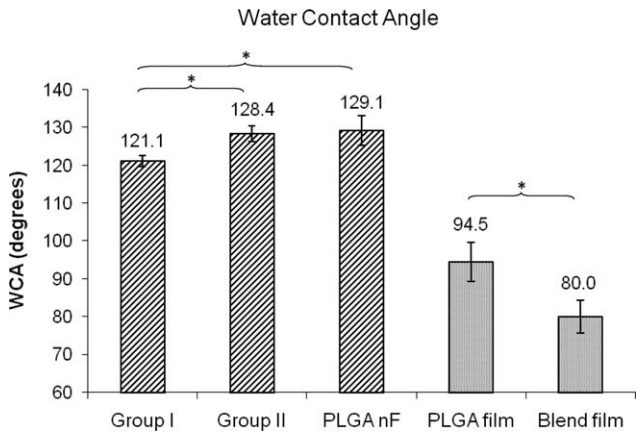

Figure 5. Surface contact angles of the different nanofibers, and of PLGA and blend films, showing that blending with proteins increased hydrophilicity.

larly, Group II (+) scaffolds had higher cell proliferation compared to Group II (−). No statistical difference was observed between Group I and Group II scaffolds. Cells cultured on TCP gave prominently higher readings compared to the various nanofibrous scaffolds (Fig. 8); this was likely the result of a higher efficiency of cell lysis and DNA extraction from culture flasks as compared to scaffolds.

Collagen production: Sircol assay

No definite trend could be observed from the Sircol assays and collagen production was similar on the various scaffolds and TCP substrate during the 2 weeks of culture (data not shown). In all the sets, the values dropped from day 3 to day 7 but showed an increase at day 14. This could be possibly because of falsely high Day 3 values resulting from proteins from unattached dead cells derived from the seeded cell population, in the assayed culture medium. As the total cell number on the different scaffolds were different on the various time points, collagen production was normalized against the respective cell

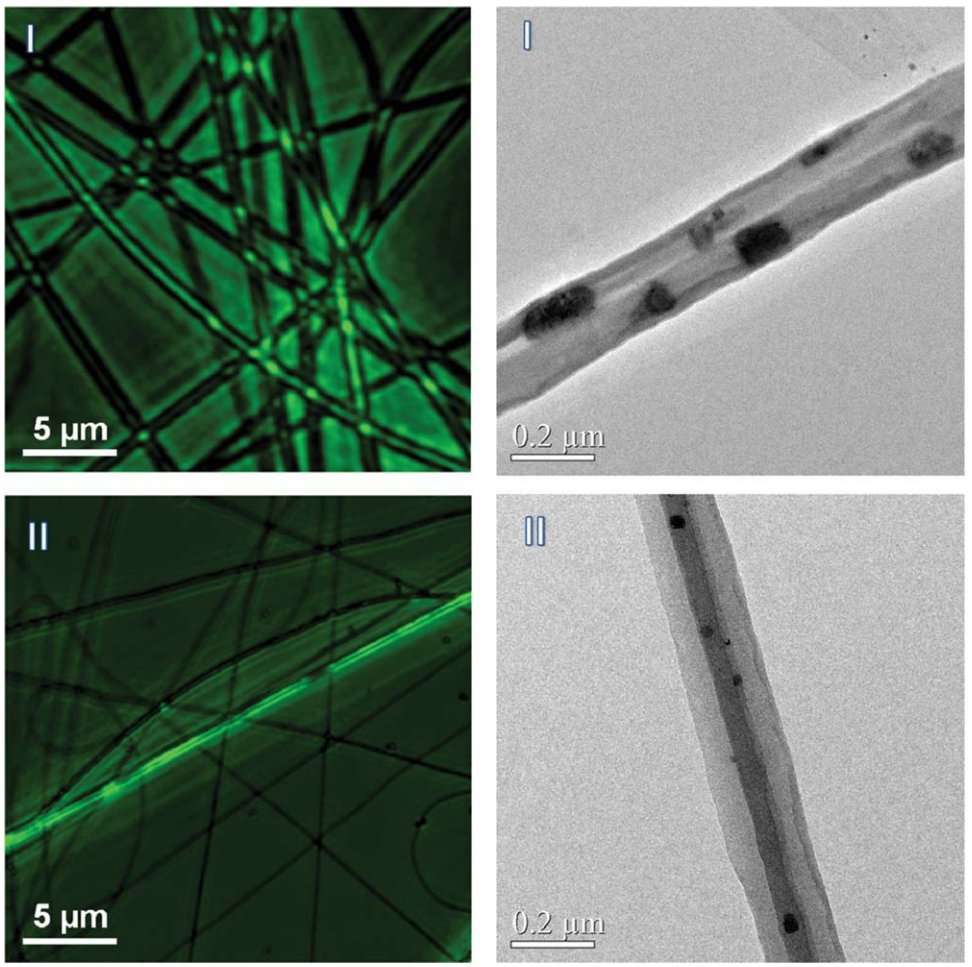

Figure 6. Different protein distribution patterns in Group I and II nanofibers observed under LSCM (FITC-conjugated BSA was used as the model protein) and TEM: random dispersion within Group I and as a uniform core within the "core-shell" Group II nanofibers. [Color figure can be viewed in the online issue, which is available at www.interscience.wiley.com.]

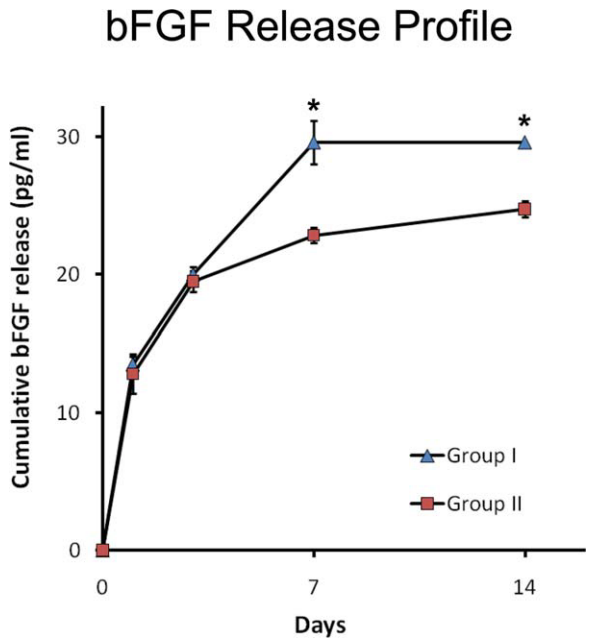

Figure 7. bFGF release profile showing prolonged release of bFGF over at least 1 week; Group II nanofibers showed a slightly prolonged release profile. [Color figure can be viewed in the online issue, which is available at www.interscience.wiley.com.]

proliferation assay values, and against the TCP value on day 3, to determine the average collagen production per cell (Fig. 9). Group I scaffolds produced showed significantly higher average collagen production on day 3, as compared to Group II scaffolds and TCP. By day 7, bFGF-releasing scaffolds showed significantly higher average collagen production [Group I (+): 53% higher, Group II (+): 47% higher] than the respective controls. All nanofibrous scaffolds had higher collagen production compared to the TCP control on day 14.

Q-RT-PCR analysis for expression of fibrous ECM proteins from BMSC

Analyses of Q-RT-PCR results (Fig. 10) by single-factor ANOVA showed upregulation of gene expression for the fibrous ECM proteins, collagen type I and fibronectin, in the BMSCs grown all nanofibrous scaffolds compared to BMSCs on TCP, at the end of one week. Collagen type I expression was lower on the Group I (+) scaffolds than on the Group I (−) control on day 7, but the scenario was reversed by day 14. Although the expression of collagen type I on the Group I (+) scaffolds increased between day 7 and day 14, that of fibronectin decreased (on all nanofibrous scaffolds). By the end of 2 weeks, Group I (+) scaffolds showed significantly higher gene expression of collagen type I and fibronectin compared to all other groups. In comparison, cells grown on Group II (+) scaffolds, surprisingly, showed lower collagen type I and fibronectin gene expression, at the end of 2 weeks, compared to TCP control. While gene expression levels were significantly higher on Group II (+) compared to Group II (−) scaffolds on day 7, there were no difference in gene expression levels at the end of 2 weeks.

DISCUSSION

Two types of polymeric nanoscaffolds capable of continued release of a bioactive growth factor over a period of 1 week were developed. It was found that both Group I and Group II scaffolds were composed of smooth continuous nanofibers, with proteins successfully incorporated in them, randomly dispersed in Group I and as a central core within Group II nanofibers. While Group I scaffolds were more hydrophilic, both groups favored BMSC attachment and cell proliferation was better on the bFGF-releasing scaffolds compared to respective controls without the growth factor. Group II scaffolds allowed a slightly longer sustained release of the encapsulated growth factor. Though total soluble collagen production was similar on the different scaffolds, the average collagen production per cell was higher on the bFGF-releasing scaffolds than their respective controls on day 7. On day 14, gene expression for collagen type I and fibronectin were better on bFGF-releasing Group I (+) scaffolds compared to their Group II counterparts, suggesting that Group I (+) scaffolds were more conducive for fibroblastic differentiation of BMSCs.

Nanofibers as vehicles for controlled delivery of bioactive molecules

In this study, it was shown that bFGF was incorporated successfully into and released gradually from electrospun nanofibers. The encapsulation efficiency and the release profile were similar for blend and coaxial nanofibers, with the growth factor being released over 1 week. Compared to blend electrospinning, the set-up for coaxial electrospinning was difficult to sterilize and required perfect alignment of the coaxial needles for continued and stable production of coaxial nanofibers. Fabrication of Group I scaffolds was thus relatively more facile than Group II scaffolds.

The potential of electrospun nanofibrous scaffolds to incorporate and release proteins like growth factors has been recently explored by several researchers.[12–15] Protein release from nanofibers has been hypothesized to be effected through a combination of passive diffusion across nanopores on the nanofiber surface and material degradation of the nanofibers.[17,20,25] Although inclusion of porogens could

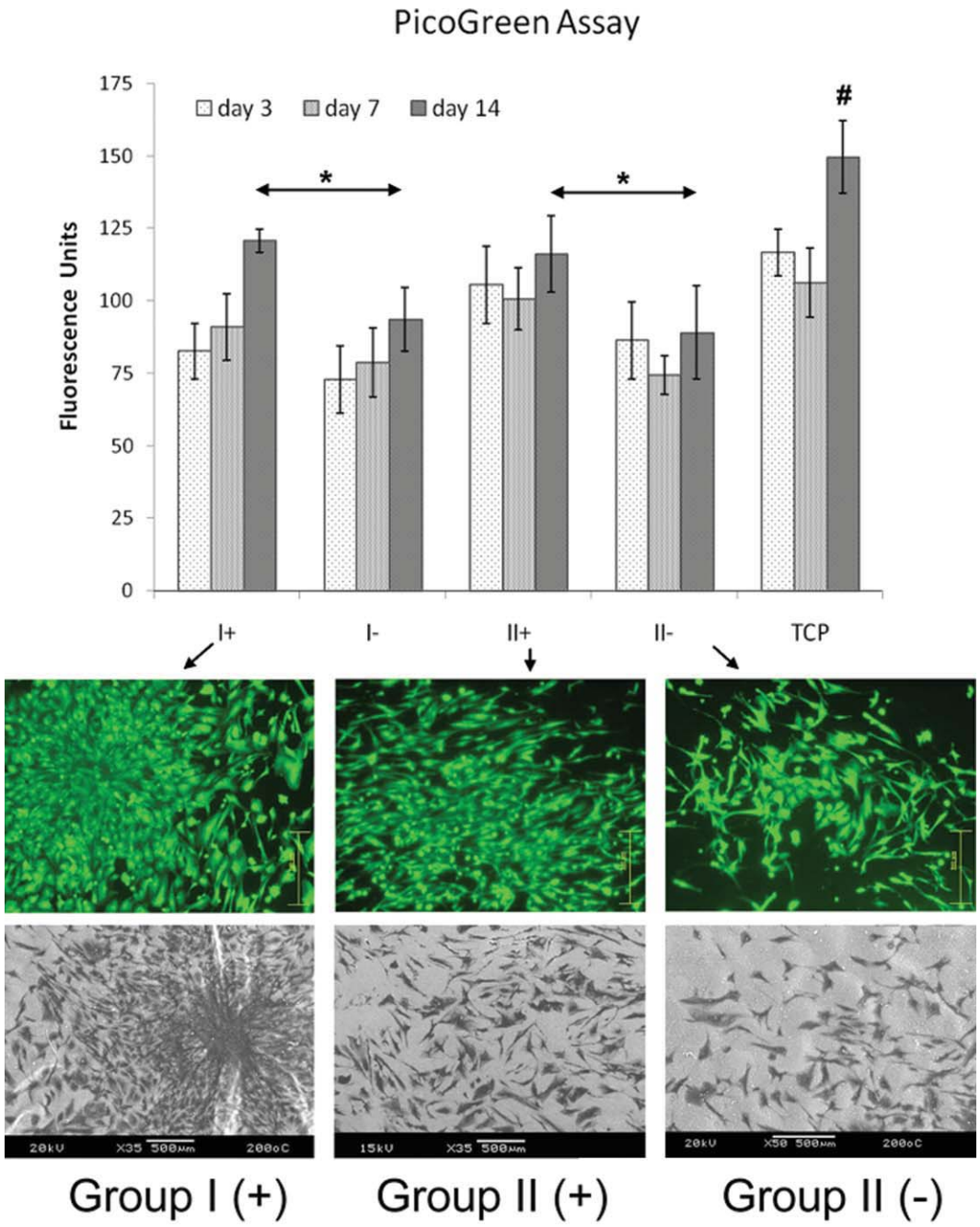

Figure 8. BMSC proliferation on various scaffolds over 2 weeks; better cell proliferation on bFGF-delivering Group I and II scaffolds, compared to scaffolds without bFGF, was demonstrated by PicoGreen assay, fluorescence microscopy after FDA staining and SEM (*, significant difference; #, apparently high cell proliferation on 2-D TCP substrate). [Color figure can be viewed in the online issue, which is available at www.interscience.wiley.com.]

increase the rate of release, small proteins have been reported to diffuse through PLGA shells created without porogens.[26] It is to be noted that electrospinning results in chain scission of PLGA molecules and increase in their rate of subsequent hydrolytic degradation, particularly in the amorphous regions.[27] Protein release from the nanofibers developed in this study is also expected to have the underlying mechanisms of diffusion and degradation. The magnitude and kinetics of protein release may thus be controlled by modifying the amount of growth factor loaded into the scaffold and the material composition of the nanofibers.[28] Both the concentration and duration of exposure to bFGF, and the presence of other growth and differentiation factors influence cell behavior[4,29,30]; by varying the dose and duration of bFGF release, as well as using a combination of growth factors, nanofibers could be further optimized for tissue engineering applications.

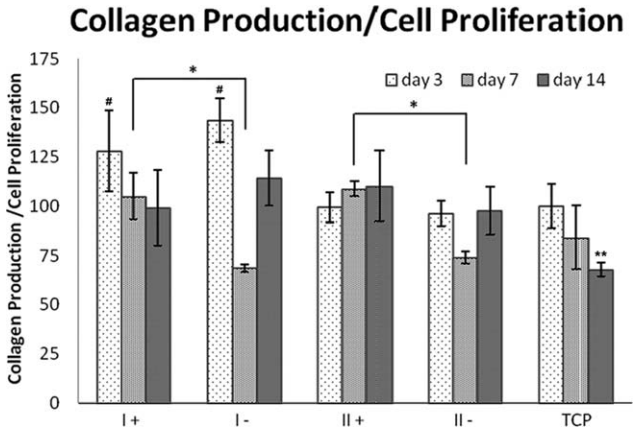

Figure 9. Normalized values of collagen production: cell proliferation on the scaffolds over 2 weeks of culture; Group I scaffolds showed higher average collagen production compared to their Group II controls on day 3 (#); bFGF-releasing scaffolds showed significantly higher (*) collagen production [Group I (+): 53% higher, Group II (+): 47% higher] than the respective controls on day 7; collagen production on all nanofibrous substrates were significantly higher than on TCP substrate on day 14 (**).

Bioactivity of the released bFGF was not determined in this study; it is expected that the bFGF, once released into the buffer, would lose bioactivity. As the release media were collected after prolonged periods of incubation, this study design precluded obtaining of reliable data on bFGF bioactivity or release efficiency (percentage of encapsulated bFGF that was released over 14 days). More frequent sampling could help in obtaining such data.

Nanofibers as biomimetic substrates for cells

The resemblance of nanofibrous substrates to the nanostructure of natural ECM, where collagen type I fibrils have similar diameters ranging between 50 and 500 nm, is postulated to facilitate cell attachment, proliferation and ECM deposition.[10,11] In this study, BMSCs demonstrated gene upregulation of fibrous ECM proteins after 7 days of culture on Group I (−) scaffolds without bFGF, indicating the contribution of nanotopographic cues from the scaffold in determining cell behavior and fate. Incorporation and release of bFGF resulted in significantly higher gene expression on Group I (+) compared to Group I (−) scaffolds on day 14, suggesting a synergistic effect of nanotopography and growth factor release on the cells.

Collagen and fibronectin showed different temporal patterns of gene expression. Collagen type I under-expression on day 7, but overexpression by day 14, on Group I (+) scaffolds suggests that high bFGF levels initially maintained BMSCs in an actively proliferating undifferentiated phenotype, while more sustained bFGF levels stimulated their fibroblastic differentiation in the 2nd week. In contrast, fibronectin showed an earlier expression profile. Fibronectin is known to regulate initial cell attachment and survival, and its downregulation in the second week is indicative of cell maturation and accumulation of collagenous ECMs.[31,32]

However, the reason behind BMSCs behaving differently on the Group II nanofibers, where the bFGF release profile was only slightly different, is not fully understood. Although physical differences (such as the observed lower surface contact angle and higher hydrophilicity in the Group I nanofibers, that govern initial protein and cell adhesion) could be a cause, it is likely that other factors like material properties (such as surface chemistry, surface energy or topography of the nanofibers) that have not been investigated in this study, might be positively influencing BMSC fate on the Group I nanofibers.

Effect of bFGF release profile on BMSC proliferation and differentiation

Inclusion of bFGF in either scaffold group resulted in increased cell proliferation. PicoGreen readings

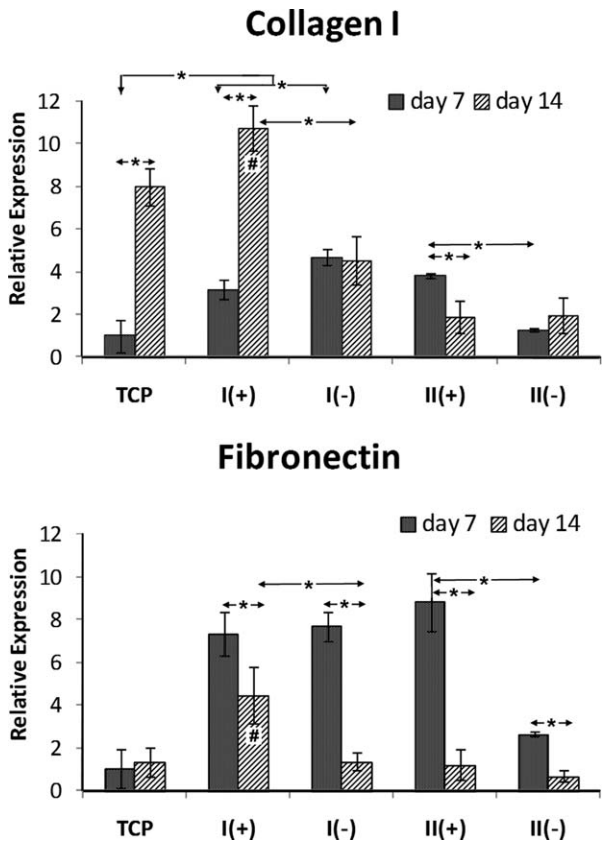

Figure 10. Q-RT-PCR analysis showing a significant gene upregulation of collagen type I and fibronectin on all nanofibrous scaffolds compared to TCP at the end of 1 week; fibronectin expression declined in the 2nd week, but after 2 weeks, Group I (+) scaffolds showed significantly higher gene expression of both fibrous proteins compared to all other groups.

obtained from cells grown on culture flasks were higher; this was likely the result of a higher efficiency of cell lysis and DNA extraction from the 2D substrate of culture flasks as compared to 3D nanofibrous scaffolds.[33] A drop in cell proliferation values was observed on both Group II (+) and (−) scaffolds on day 7. This could be because of the fact that the growth factor release from the coaxial Group II (+) scaffolds was not sufficiently high to stimulate cell proliferation. On the contrary, a faster release of bFGF from the Group I (+) scaffolds could sustain consistent cell proliferation.

Fibroblastic differentiation of BMSCs on Group I (+) scaffolds, indicated by significant gene upregulation of fibrous ECM proteins, also suggests that bFGF released over 1 week was sufficient and more effective that a more prolonged release. Several injured connective tissues have increased tissue levels of bFGF only during the 1st week of injury.[34–36] The Group I (+) scaffold could thus "biomimick" the ECM of such injured tissues in both structure and function by providing a nanofibrous topography as well as a week-long supply of bioactive bFGF to the resident cells. Usual *in vitro* culture conditions using 5–15% FBS have bFGF levels of 15–45 pg/mL.[37] Previous studies have shown that BMSCs grown in culture medium supplemented with 0.1–10 ng/mL of bFGF and replenished twice weekly resulted in increased proliferation, self-renewal and differentiation into fibroblastic cells.[4,38] However, in this study, a sustained bFGF level in the concentration of picograms was shown to be sufficient to induce the same effects.

This study demonstrated the effect of sustained release of a single growth factor from electrospun nanofibers. Stem cell differentiation usually depends on a combination of growth and differentiation factors. By modifying the nanofibrous substrate as well as by introducing different combination of growth factors, and varying their dose and duration of release, scaffolds systems could optimized for different tissue engineering applications. As nanofibrous substrates alone do not possess sufficient strength to mechanically support the regeneration of injured tissues, nanofibers have been combined with microfibrous scaffolds to create hybrid scaffolds for tendon/ligament tissue engineering applications[10]; bioactive nanofibers developed in this study could be used to improve such hybrid scaffolds.

CONCLUSIONS

Polymeric nanoscaffolds capable of continued release of bioactive growth factors, with different release profiles and surface hydrophilicity, are presented. The combination of a nanofibrous substrate and sustained growth factor release could positively influence cell fate. It has been shown that between Group I and Group II scaffolds, Group I scaffolds released the incorporated bFGF in a bioactive form over 1 week, were more hydrophilic, favored BMSC attachment and, particularly, proliferation and differentiation into a fibroblastic lineage. However, Group II scaffolds could sustain the growth factor release up to 2 weeks. By choosing the appropriate biomaterial for nanofiber fabrication and the relevant growth factor(s), it would be possible to fabricate bioactive nanofibers suitable for different tissue engineering applications.

References

1. Whitaker MJ, Quirk RA, Howdle SM, Shakesheff KM. Growth factor release from tissue engineering scaffolds. J Pharm Pharmacol 2001;53:1427–1437.
2. Bhattarai SR, Bhattarai N, Yi HK, Hwang PH, Cha DI, Kim HY. Novel biodegradable electrospun membrane: Scaffold for tissue engineering. Biomaterials 2004;25:2595–2602.
3. Li WJ, Tuli R, Huang X, Laquerriere P, Tuan RS. Multilineage differentiation of human mesenchymal stem cells in a three-dimensional nanofibrous scaffold. Biomaterials 2005;26:5158–5166.
4. Hankemeier S, Keus M, Zeichen J, Jagodzinski M, Barkhausen T, Bosch U, Krettek C, Van Griensven M. Modulation of proliferation and differentiation of human bone marrow stromal cells by fibroblast growth factor 2: Potential implications for tissue engineering of tendons and ligaments. Tissue Eng 2005;11:41–49.
5. Gospodarowicz D. Fibroblast growth factor. Chemical structure and biologic function. Clin Orthop Relat Res 1990;257:231–248.
6. Goldfarb M. Fibroblast growth factor homologous factors: Evolution, structure, and function. Cytokine Growth Factor Rev 2005;16:215–220.
7. Goh JC, Ouyang HW, Teoh SH, Chan CK, Lee EH. Tissue-engineering approach to the repair and regeneration of tendons and ligaments. Tissue Eng 2003;9(Suppl 1):S31–S44.
8. Ge Z, Goh JC, Wang L, Tan EP, Lee EH. Characterization of knitted polymeric scaffolds for potential use in ligament tissue engineering. J Biomater Sci Polym Ed 2005;16:1179–1192.
9. Ouyang HW, Toh SL, Goh J, Tay TE, Moe K. Assembly of bone marrow stromal cell sheets with knitted poly (L-lactide) scaffold for engineering ligament analogs. J Biomed Mater Res B Appl Biomater 2005;75:264–271.
10. Sahoo S, Ouyang H, Goh JC, Tay TE, Toh SL. Characterization of a novel polymeric scaffold for potential application in tendon/ligament tissue engineering. Tissue Eng 2006;12:91–99.
11. Sahoo S, Goh JCH, Toh SL. Development of hybrid polymer scaffolds for potential applications in ligament and tendon tissue engineering. Biomed Mater 2007;2:169–173.
12. Chew SY, Wen J, Yim EK, Leong KW. Sustained release of proteins from electrospun biodegradable fibers. Biomacromolecules 2005;6:2017–2024.
13. Casper CL, Yamaguchi N, Kiick KL, Rabolt JF. Functionalizing electrospun fibers with biologically relevant macromolecules. Biomacromolecules 2005;6:1998–2007.
14. Liao IC, Chew SY, Leong KW. Aligned core-shell nanofibers delivering bioactive proteins. Nanomedicine 2006;1:465–471.

15. Li C, Vepari C, Jin HJ, Kim HJ, Kaplan DL. Electrospun silk-BMP-2 scaffolds for bone tissue engineering. Biomaterials 2006;27:3115–3124.
16. Zhang YZ, Wang X, Feng Y, Li J, Lim CT, Ramakrishna S. Coaxial electrospinning of (fluorescein isothiocyanate-conjugated bovine serum albumin)-encapsulated poly(epsilon-caprolactone) nanofibers for sustained release. Biomacromolecules 2006;7:1049–1057.
17. Jiang H, Hu Y, Li Y, Zhao P, Zhu K, Chen W. A facile technique to prepare biodegradable coaxial electrospun nanofibers for controlled release of bioactive agents. J Controlled Release 2005;108:237–243.
18. Zhang YZ, Venugopal J, Huang ZM, Lim CT, Ramakrishna S. Characterization of the surface biocompatibility of the electrospun PCL-collagen nanofibers using fibroblasts. Biomacromolecules 2005;6:2583–2589.
19. Huang ZM, He CL, Yang A, Zhang Y, Han XJ, Yin J, Wu Q. Encapsulating drugs in biodegradable ultrafine fibers through co-axial electrospinning. J Biomed Mater Res A 2006;77: 169–179.
20. Jiang H, Hu Y, Zhao P, Li Y, Zhu K. Modulation of protein release from biodegradable core-shell structured fibers prepared by coaxial electrospinning. J Biomed Mater Res B Appl Biomater 2006;79:50–57.
21. Gupta RK, Chang A-C, Griffin P, Rivera R, Guo Y-Y, Siber GR. Determination of protein loading in biodegradable polymer microspheres containing tetanus toxoid. Vaccine 1997;15: 672–678.
22. Cooper JA, Bailey LO, Carter JN, Castiglioni CE, Kofron MD, Ko FK, Laurencin CT. Evaluation of the anterior cruciate ligament, medial collateral ligament, achilles tendon and patellar tendon as cell sources for tissue-engineered ligament. Biomaterials 2006;27:2747–2754.
23. Egerton RF, Li P, Malac M. Radiation damage in the TEM and SEM. Micron 2004;35:399–409.
24. Van De Weert M, Van 'T Hof R, Van Der Weerd J, Heeren RM, Posthuma G, Hennink WE, Crommelin DJ. Lysozyme distribution and conformation in a biodegradable polymer matrix as determined by FTIR techniques. J Controlled Release 2000;68:31–40.
25. Ramakrishna S, Fujihara K, Teo W-E, Yong T, Ma Z, Ramaseshan R. Electrospun nanofibers: Solving global issues. Mater Today 2006;9:40–50.
26. Kim BS, Oh JM, Kim KS, Seo KS, Cho JS, Khang G, Lee HB, Park K, Kim MS. BSA-FITC-loaded microcapsules for in vivo delivery. Biomaterials 2009;30:902–909.
27. Zong X, Ran S, Kim KS, Fang D, Hsiao BS, Chu B. Structure and morphology changes during in vitro degradation of electrospun poly(glycolide-*co*-lactide) nanofiber membrane. Biomacromolecules 2003;4:416–423.
28. Zisch AH, Lutolf MP, Hubbell JA. Biopolymeric delivery matrices for angiogenic growth factors. Cardiovasc Pathol 2003;12:295–310.
29. Moreau JE, Chen J, Bramono DS, Volloch V, Chernoff H, Vunjak-Novakovic G, Richmond JC, Kaplan DL, Altman GH. Growth factor induced fibroblast differentiation from human bone marrow stromal cells in vitro. J Orthop Res 2005;23:164–174.
30. Moreau JE, Chen J, Horan RL, Kaplan DL, Altman GH. Sequential growth factor application in bone marrow stromal cell ligament engineering. Tissue Eng 2005;11:1887–1897.
31. Chen J, Horan RL, Bramono D, Moreau JE, Wang Y, Geuss LR, Collette AL, Volloch V, Altman GH. Monitoring mesenchymal stromal cell developmental stage to apply on-time mechanical stimulation for ligament tissue engineering. Tissue Eng 2006;12:3085–3095.
32. Venugopal JR, Zhang Y, Ramakrishna S. In vitro culture of human dermal fibroblasts on electrospun polycaprolactone collagen nanofibrous membrane. Artif Organs 2006;30:440–446.
33. Ng KW, Leong DT, Hutmacher DW. The challenge to measure cell proliferation in two and three dimensions. Tissue Eng 2005;11:182–191.
34. Kobayashi M, Itoi E, Minagawa H, Miyakoshi N, Takahashi S, Tuoheti Y, Okada K, Shimada Y. Expression of growth factors in the early phase of supraspinatus tendon healing in rabbits. J Shoulder Elbow Surg 2006;15:371–377.
35. Berglund M, Reno C, Hart DA, Wiig M. Patterns of mRNA expression for matrix molecules and growth factors in flexor tendon injury: Differences in the regulation between tendon and tendon sheath. J Hand Surg (Am) 2006;31:1279–1287.
36. Wurgler-Hauri CC, Dourte LM, Baradet TC, Williams GR, Soslowsky LJ. Temporal expression of 8 growth factors in tendon-to-bone healing in a rat supraspinatus model. J Shoulder Elbow Surg 2007;16(Suppl):S198–S203.
37. Ayache S, Panelli MC, Byrne KM, Slezak S, Leitman SF, Marincola FM, Stroncek DF. Comparison of proteomic profiles of serum, plasma, and modified media supplements used for cell culture and expansion. J Transl Med 2006;4:40–51.
38. Tsutsumi S, Shimazu A, Miyazaki K, Pan H, Koike C, Yoshida E, Takagishi K, Kato Y. Retention of multilineage differentiation potential of mesenchymal cells during proliferation in response to FGF. Biochem Biophys Res Commun 2001;288:413–419.